The EMBO Journal Vol.16 No.8 pp.1876–1887, 1997

Structural basis for the recognition of regulatory subunits by the catalytic subunit of protein phosphatase 1

Marie-Pierre Egloff, Deborah F.Johnson[1], Greg Moorhead[1], Patricia T.W.Cohen[1], Philip Cohen[1] and David Barford[2]

Laboratory of Molecular Biophysics, University of Oxford, Rex Richards Building, South Parks Road, Oxford OX1 3QU and [1]MRC Protein Phosphorylation Unit, Department of Biochemistry, University of Dundee, Dundee DD1 4HN, UK

[2]Corresponding author

The diverse forms of protein phosphatase 1 *in vivo* result from the association of its catalytic subunit (PP1c) with different regulatory subunits, one of which is the G-subunit (G_M) that targets PP1c to glycogen particles in muscle. Here we report the structure, at 3.0 Å resolution, of PP1c in complex with a 13 residue peptide ($G_{M[63–75]}$) of G_M. The residues in $G_{M[63–75]}$ that interact with PP1c are those in the Arg/Lys–Val/Ile–Xaa–Phe motif that is present in almost every other identified mammalian PP1-binding subunit. Disrupting this motif in the $G_{M[63–75]}$ peptide and the $M_{110[1–38]}$ peptide (which mimics the myofibrillar targeting M_{110} subunit in stimulating the dephosphorylation of myosin) prevents these peptides from interacting with PP1. A short peptide from the PP1-binding protein p53BP2 that contains the RVXF motif also interacts with PP1c. These findings identify a recognition site on PP1c, invariant from yeast to humans, for a critical structural motif on regulatory subunits. This explains why the binding of PP1 to its regulatory subunits is mutually exclusive, and suggests a novel approach for identifying the functions of PP1-binding proteins whose roles are unknown.

Keywords: protein phosphatase 1/recognition motif/recognition site/regulatory subunits/X-ray crystallography

Introduction

The reversible phosphorylation of proteins regulates most aspects of cell life. About a third of all mammalian proteins are now thought to contain covalently bound phosphate and, since protein kinases and phosphatases probably account for ~2–3% of all human gene products (Hunter, 1995), many of these enzymes must typically phosphorylate/dephosphorylate numerous proteins *in vivo*. However, it is becoming increasingly clear that some protein kinases and phosphatases do not find their physiological substrates by simple diffusion within cells and that they frequently are directed to particular loci in the vicinity of their substrates by interaction with targeting subunits. In this way, the actions of protein kinases and phosphatases with inherently broad specificities are restricted and their properties tailored to the needs of a particular subcellular location, organelle or process (reviewed in Hubbard and Cohen, 1993; Faux and Scott, 1996).

The paradigm for the targeting subunit concept is protein phosphatase-1 (PP1), one of the major serine/threonine-specific protein phosphatases of eukaryotic cells (Stralfors *et al.*, 1985). This enzyme is involved in controlling diverse cellular functions including glycogen metabolism, muscle contraction, the exit from mitosis and the splicing of RNA (Cohen, 1989; Mermoud *et al.*, 1992; Shenolikar, 1994; Wera and Hemmings, 1995). These different processes appear to be regulated by distinct PP1 holoenzymes in which the same catalytic subunit (PP1c) is complexed to different targeting or regulatory subunits. The latter class of subunits act to confer *in vivo* substrate specificity not only by directing PP1c to the subcellular loci of its substrates, but also by enhancing or suppressing its activity towards different substrates. In addition, the regulatory subunits allow the activity of PP1 to be modulated by reversible protein phosphorylation and second messengers in response to extracellular stimuli.

Several mammalian PP1c targeting subunits have been isolated and characterized, including the G_M subunit that targets PP1c to both the glycogen particles and sarcoplasmic reticulum of striated muscle (Tang *et al.*, 1991), the G_L subunit that targets PP1c to liver glycogen (Doherty *et al.*, 1995; Moorhead *et al.*, 1995), the M_{110} subunits responsible for the association of PP1c with the myofibrils of skeletal muscle (Alessi *et al.*, 1992; Moorhead *et al.*, 1994) and smooth muscle (Alessi *et al.*, 1992; Chen *et al.*, 1994), the p53-binding protein p53BP2 (Helps *et al.*, 1995) and the nuclear protein NIPP-1 (Jagiello *et al.*, 1995; Van Eynde *et al.*, 1995). PP1c is also reported to interact with other mammalian proteins such as the retinoblastoma gene product (Durfee *et al.*, 1993), an RNA-splicing factor (Hirano *et al.*, 1996), ribosomal protein L5 (Hirano *et al.*, 1995) and RIPP-1 (Beullens *et al.*, 1996), a 110 kDa nuclear protein yet to be identified (Jagiello *et al.*, 1995) and small cytosolic proteins, inhibitor-1, DARPP-32 and inhibitor-2 (reviewed in Cohen, 1989, 1992; Hubbard and Cohen, 1993). Moreover, a number of distinct PP1 regulatory subunits have been identified in yeast (reviewed by Stark, 1996). It seems likely that many further PP1 targeting subunits remain to be identified, and the exploitation of powerful new techniques such as microcystin–Sepharose affinity chromatography (Moorhead *et al.*, 1994) and the yeast two-hybrid system (Helps *et al.*, 1995) are accelerating the rate at which new PP1 targeting subunits are being discovered.

Each form of PP1c that has been isolated contains just one PP1c-binding subunit, implying that the interaction of different targeting subunits with PP1c is mutually exclusive and that the binding site(s) for different targeting subunits is (are) identical or overlapping. This would

suggest that most, if not all, targeting subunits have a common PP1c-binding motif. Surprisingly, elucidation of the amino acid sequences of a number of targeting subunits initially failed to reveal significant sequence similarities common to all these proteins. However, comparison of G_M and G_L identified three short highly conserved regions, one being residues 63–86 of G_M (Doherty *et al.*, 1995). Peptides comprising residues 63–93, 63–80 and 63–75 of G_M were therefore synthesized and found to bind to PP1c (Johnson *et al*., 1996).

We then sought to identify the region of the M_{110} subunit that binds to PP1c by deletion analysis and peptide synthesis. These studies led to the finding that the N-terminal 38 residues ($M_{110[1–38]}$) mimic the intact M_{110} subunit in enhancing the rate at which PP1c dephosphorylated the 20 kDa myosin light chain (MLC_{20}) subunit of smooth muscle myosin (Johnson *et al.*, 1996). The finding that $G_{M[63–93]}$ disrupted the interaction between PP1c and the M_{110} subunit and prevented M_{110} from enhancing the MLC_{20} phosphatase activity of PP1c implies that the binding of M_{110} and G_M to PP1c is mutually exclusive.

To understand the basis for the recognition by PP1c of regulatory subunits, and peptides derived from these subunits, we have co-crystallized a complex of PP1c with the $G_{M[63–75]}$ peptide and determined the structure at 3.0 Å resolution. These experiments have demonstrated that residues 64–69 of the peptide are bound in an extended conformation to a hydrophobic channel within the C-terminal region of PP1c. The residues in $G_{M[63–75]}$ that interact with PP1c lie in an Arg/Lys–Val/Ile–Xaa–Phe motif common to $M_{110[1–38]}$ and almost all known mammalian PP1-binding proteins. Substituting Val or Phe by Ala in the $G_{M[63–75]}$ peptide, and deleting the VXF motif from the $M_{110[1–38]}$ peptide, abolished the ability of both peptides to interact with PP1c. Moreover, a peptide from p53BP2 that contains the RVXF motif also bound to PP1c. These findings identify a recognition site on PP1c for a critical structural motif involved in the interaction with its targeting subunits.

Results and discussion

Structure determination

Crystallographic data to 3.0 Å were measured at the ESRF beam-line BL4 at Grenoble and at PX9.6, Daresbury (Table I). The relatively high merging *R*-factors and low I/σI values of the crystallographic data result from the weak diffraction observed from the PP1–$G_{M[63–75]}$ peptide complex crystals. This is attributable to both the small crystal size (~25 μm×25 μm×5 μm) and long *c*-axis of the unit cell. In addition, the high X-ray photon dose required to obtain usable diffraction images resulted in X-ray radiation damage to the crystals, despite being maintained at a temperature of 100 K during the course of the experiment. The structure was solved by the molecular replacement method using as a search model the 2.5 Å refined coordinates of PP1c (Egloff *et al.*, 1995). Phases obtained from a single cycle of simulated annealing refinement of the protein coordinates alone using X-PLOR (Brünger, 1992), and improved by 2-fold non-crystallographic symmetry averaging and solvent flattening, were used to calculate an electron density map. This map revealed clear density corresponding to residues Val66′, Ser67′ and Phe68′ of the G_M peptide (where the prime denotes residues of the peptide) and provided a starting point for further refinement of the PP1–$G_{M[63–75]}$ peptide complex. The final model of the complex was refined at 3.0 Å resolution with a crystallographic *R*-factor of 0.22 and *R*-free of 0.31 (Figure 1). The two molecules of PP1c within the asymmetric unit are similar with a root-mean-square deviation (r.m.s.d.) between main-chain atoms of 0.6 Å. Residues 6–299 and 8–297 from molecules 1 and 2, respectively, are visible in the electron density map. Similar to the structures of native PP1γ1 (Egloff *et al.*, 1995) and PP1α in complex with microcystin LR (Goldberg *et al.*, 1995), residues C-terminal to 299 are disordered.

Table I. Crystallographic data and refinement statistics

Crystallographic data	
Space group	$P4_12_12$
Unit cell parameters (Å)	$a = b = 62.50$; $c = 361.30$
Molecules per asymmetric unit (*N*)	2
Crystals used during data collection (*N*)	4
Temperature (K)	100
Total measured reflections (*N*)	290 671
Unique reflections (*N*)	15 509
Mean $I/\sigma(I)$	7.5
Completeness (%)	87
R-merge[a] (%)	14.7
Refinement statistics	
Reflections used for refinement (*N*)	13 078
Resolution range (Å)	8.0–3.0
R_{cryst}[b] (work)	0.223
R_{cryst} (free)	0.308
Protein and peptide atoms (*N*)	5861
Water molecules (*N*)	14
R.m.s.d. from ideal bond lengths (Å)	0.012
R.m.s.d. from ideal angles (°)	1.863

[a]*R*-merge: $\Sigma_h\Sigma_i|I_{(h)}–I_{i(h)}|\Sigma_h\Sigma_i I_{i(h)}$ where $I_{i(h)}$ and $I_{(h)}$ are the ith and mean measurements of the intensity of reflection h.
[b]R_{cryst}: $\Sigma_h|F_o–F_c|\Sigma_h F_o$ where F_o and F_c are the observed and calculated structure factor amplitudes of reflection h.

Overall structure of PP1

The conformation of PP1c in the PP1–$G_{M[63–75]}$ peptide complex is virtually identical to that of native PP1c in complex with tungstate (Egloff *et al.*, 1995) with an r.m.s.d. between equivalent main-chain atoms of 1.0 Å. PP1c is folded into a single elliptical domain consisting of a central β-sandwich of two mixed β-sheets surrounded on one side by seven α-helices and on the other by a subdomain consisting of three α-helices and a three-stranded mixed β-sheet (Figure 2A). The interface of the three β-sheets at the top of the β-sandwich creates a shallow catalytic site channel. Three loops connecting β-strands with α-helices within a β-α-β-α-β motif in sheet 1 (strand order β4-β3-β2-β13-β14) together with loops emanating from the opposite β-sheet (sheet 2; strand order β1-β5-β6-β10-β12-β11) provide the catalytic site residues. The catalytic site of PP1 contains a binuclear metal site consisting of Mn^{2+} and Fe^{2+} (Egloff *et al.*, 1995) and, in the PP1–$G_{M[63–75]}$ peptide complex, oxygen atoms of a sulfate ion of crystallization coordinate both metal ions,

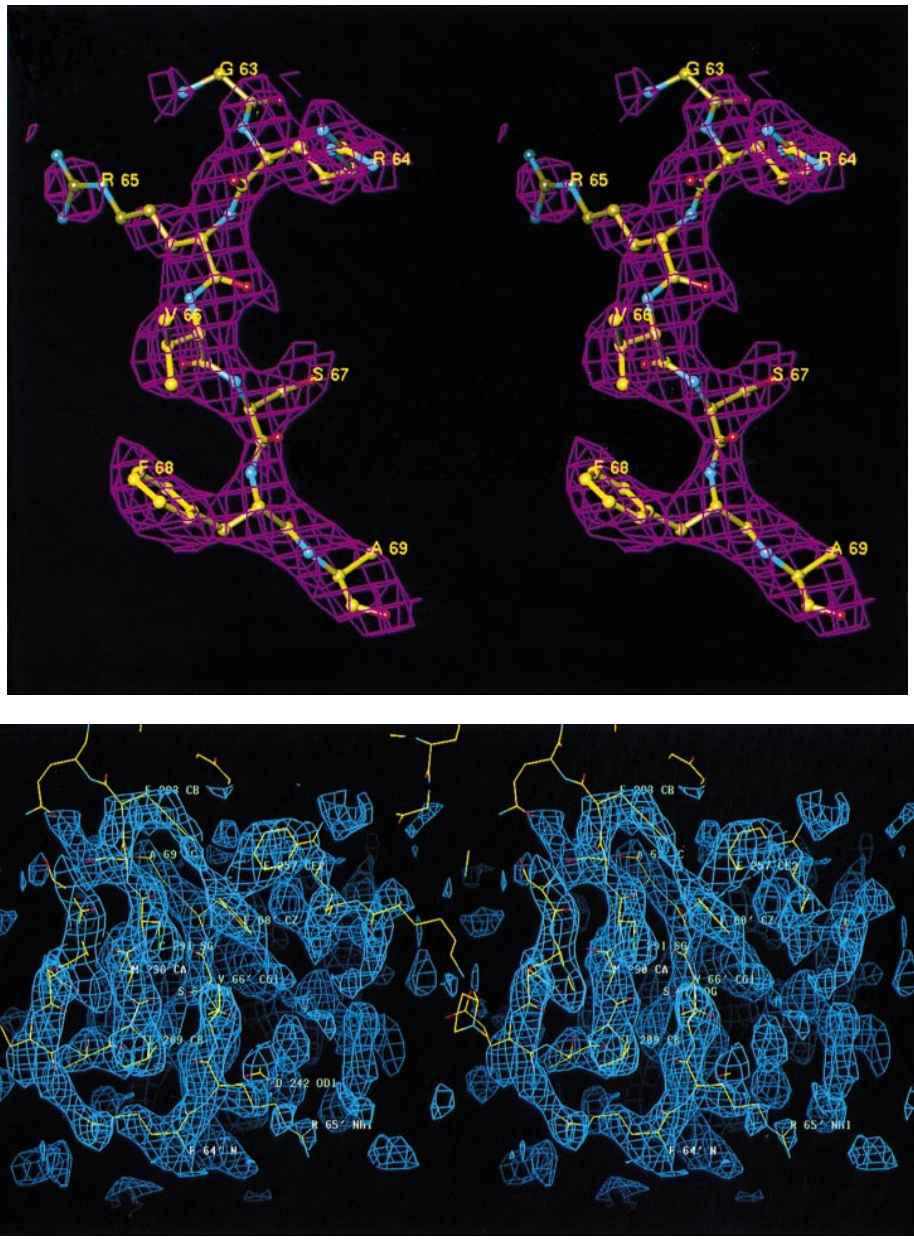

Fig. 1. Stereo views of electron density maps. (**A**) Electron density corresponding to residues Gly63–Ala69 of the $G_{M[63–75]}$ peptide. The map was calculated using $3F_o–2F_c$ coefficients and phases calculated from the final refined model. (**B**) Electron density map of the $G_{M[63–75]}$ peptide and corresponding region of PP1c. Displayed using TURBO-FRODO (Roussel and Cambillau, 1992).

similar to what is seen in the PP1–tungstate (Egloff *et al.*, 1995) and PP2B–phosphate complexes (Griffith *et al.*, 1995).

PP1c–$G_{M[63–75]}$ peptide interactions

Six residues of the $G_{M[63–75]}$ peptide (Arg64′–Ala69′) are clearly visible in the electron density map of the complex of molecule 2; the remaining residues are not visible and are assumed to be disordered (Figure 1). Density is not visible for Arg64′ of the peptide bound to molecule 1, otherwise equivalent residues of the peptide are similar within the two complexes. The six residues (RRVSFA) of the $G_{M[63–75]}$ peptide in complex 2 adopt an extended conformation and bind to a hydrophobic channel on the protein surface with dimensions 25 Å×10 Å that is formed at the interface of the two β-sheets of the β-sandwich opposite to the catalytic site channel and is therefore remote from the catalytic site (Figure 2A and B). This site differs from the position of the regulatory B-subunit binding site of the PP2B catalytic subunit (Griffith *et al.*, 1995; Kissenger *et al.*, 1995). The location of a regulatory subunit-binding site at a region distinct from the catalytic site of PP1c is also consistent with the discovery that PP1c attached to microcystin–Sepharose affinity columns maintains an intact regulatory subunit-binding site (Moorhead *et al.*, 1994).

The residues that form this channel occur on three regions of PP1c, namely: (i) the N-terminus of β5 and the β5/β6 loop of sheet 2; (ii) the three edge β-strands of sheet 2: β10, β12 and β11; and (iii) β13, the β13/β14 loop and β14 of the edge of sheet 1 (Figure 2A). The total solvent-accessible surface area buried on formation

of the complex is 980 Å^2. Three residues of the peptide (Ser67′–Ala69′) form a β-strand which is incorporated into β-sheet 1 of PP1c as a sixth β-strand parallel to the N-terminus of the edge β-strand, β14 (residues Leu289–Leu296) (Figure 2C). Main-chain atoms of Ser67′ and Ala69′ form H-bonds to the main-chain atoms of residues of β14. In addition, the main-chain nitrogen of Val66′ forms a H-bond with the side chain of Asp242. Other polar interactions include the guanidinium group of Arg64′ with the main-chain carbonyl of Glu287 and a salt bridge to the side chain of Asp166. Both Asp166 and Asp242 are invariant in mammalian PP1 isoforms. A water molecule bridges the main-chain carbonyl of Arg65′ and side-chain hydroxyl of Ser67′ with the main-chain carbonyl of Thr288 of PP1c (Figure 2C). A notable feature of the peptide-binding site is the presence of a negatively charged region created by seven acidic residues (with one Lys residue) surrounding the hydrophobic channel at the N-terminus of the peptide in the vicinity of Arg64′ and Arg65′ that includes Asp166 and Asp242 (Figure 2D). This would suggest a favourable electrostatic environment for the side chains of Arg64′ and Arg65′.

The predominant interactions between the peptide and PP1c involve hydrophobic contacts between the side chains of Val66′ and Phe68′ and solvent-exposed, invariant, hydrophobic residues of PP1c that form the hydrophobic channel (Figure 2C and E). In particular, the binding site for the side chain of Val 66′ is formed from the side chains of Ile169, Leu243, Leu289 and Cys291, whereas that for the side chain of Phe68′ is formed from the side chains of Phe257, Cys291 and Phe293. Details of peptide–PP1c contacts are given in Table II. The structure of the $G_{M[63–75]}$ peptide-binding site is likely to be conserved in other forms of PP1 from diverse species. Each hydrophobic residue of PP1c that interacts with the Val66′ and Phe68′ residues of the $G_{M[63–75]}$ peptide is invariant, and the acidic residues that surround the N-terminus of the peptide-binding site are highly conserved amongst all isoforms of PP1 from species as diverse as yeast, *Drosophila*, mammals and higher plants (Barton *et al.*, 1994). However, since these residues are not conserved within the PP2A and PP2B sequences, these proteins will not recognize PP1 regulatory subunits.

The mode of interaction between PP1c and the $G_{M[63–75]}$ peptide is similar to that observed in complexes of phosphotyrosine-binding (PTB) domains (Zhou *et al.*, 1995) and PDZ domains (Doyle *et al.*, 1996) with their cognate peptide ligands. In these complexes, short peptides of 4–6 residues engage the protein by forming anti-parallel hydrogen bonding interactions with edge β-strands that occur within a β-barrel. The peptide binding sites occur within hydrophobic channels created at the interface of secondary structural elements, namely a β-sheet and an α-helix. For PP1c the two secondary structural elements are two β-sheets. Formation of H-bonds between edge β-strands is observed at protein interfaces within a number of protein–protein complexes. For example, the streptococcal protein-G domain interaction with the C_H domain of IgG (Derrick and Wigley, 1992); the Ras-binding domain of Raf kinase with Rap1A (Nassar *et al.*, 1995) and the interaction of $p27^{Kip1}$ with Cdk2 within a ternary $p27^{Kip1}$–cyclin A–Cdk2 complex (Russo *et al.*, 1996).

Presence of an (R/K)(V/I)XF motif in other PP1c regulatory proteins

Over a dozen regulatory subunits of PP1c are now known which appear to bind to PP1c in a mutually exclusive manner that suggests an overlapping binding site or sites. Although sequence comparisons initially revealed little overall similarity between different PP1 targeting subunits, we found that M_{110} and p53BP2 could be aligned in the region of residues 774–900 of p53BP2 (Naumovski and Cleary, 1996), that binds to PP1c (Helps *et al.*, 1995). Comparison of $p53BP2_{[774–900]}$ and $M_{110[13–137]}$ aligned the two ankyrin repeats in p53BP2 with the second and third ankyrin repeats of M_{110} and identified a conserved motif (R/K)VKF (residues 35–38 of M_{110} and residues 798–801 of p53BP2) preceding the ankyrin repeats. This sequence is similar to the RVSF motif found in $G_{M[63–75]}$ and the homologous region of G_L. The motif is also the last four residues of the peptide $M_{110[1–38]}$ which was shown previously to bind to PP1c (Johnson *et al.*, 1996; Figure 3A). Moreover, a 32 residue peptide from p53BP2 (residues 780–811), which contains this motif, disrupted the interaction of the M_{110} subunit with PP1c, as shown by a decrease in the rate of dephosphorylation of the MLC_{20} subunit of smooth muscle myosin and by an increase in the rate of dephosphorylation of glycogen phosphorylase (Figure 4A). This peptide also disrupted the interaction of the G_L subunit with PP1c, as shown by an increase in the rate of dephosphorylation of glycogen phosphorylase (Figure 4B). This result indicates that the RVKF sequence in p53BP2 is important in the interaction with PP1c. Inspection of the sequences of other mammalian PP1-binding proteins also revealed an (R/K)(V/I)XF motif (Figure 3A), which was present in fragments of NIPP-1 (Beullens *et al.*, 1992; Van Eynde *et al.*, 1995) and an RNA splicing factor (Hirano *et al.*, 1996), known to interact with PP1c.

In further support of the notion of a common PP1c recognition motif present within PP1-binding proteins, previous studies had revealed that the sequence KIQF (similar to the R/KVXF motif) at the N-terminus of protein inhibitor 1 and its homologue DARPP-32 (Figure 3A) is necessary for mediating the inhibition of PP1c by these proteins. Loss of Ile10 of the KIQF motif of inhibitor 1 disrupts the inhibitory effects on PP1c by phosphoinhibitor-1 (Aitken and Cohen, 1982; Endo *et al.*, 1996) and the binding of either dephosphoinhibitor-1 or phosphoinhibitor-1 to PP1c (Endo *et al.*, 1996). A similar result was found on disrupting the equivalent residue (Ile9) of DARPP-32 (Hemmings *et al.*, 1990; Desdouits *et al.*, 1995). These results were interpreted to indicate that inhibitor-1 and DARPP-32 bind to PP1 through two low affinity binding sites, one that encompasses the sequence KIQF and another which includes the phosphorylated Thr residue (35 in I-1, 34 in DARPP-32) and which presumably binds at the catalytic site. Analysis of the PP1–$G_{M[63–75]}$ peptide complex structure suggests that an isoleucine residue could be accommodated readily within the peptide-binding site in place of Val66′ such that the additional methyl group on Ile compared with Val would contribute to favourable van der Waals interactions between the peptide and Leu243 and Cys291 of PP1. More bulky hydrophobic residues such as Leu, Met and Phe cannot be accommodated, however. It is interesting to note that,

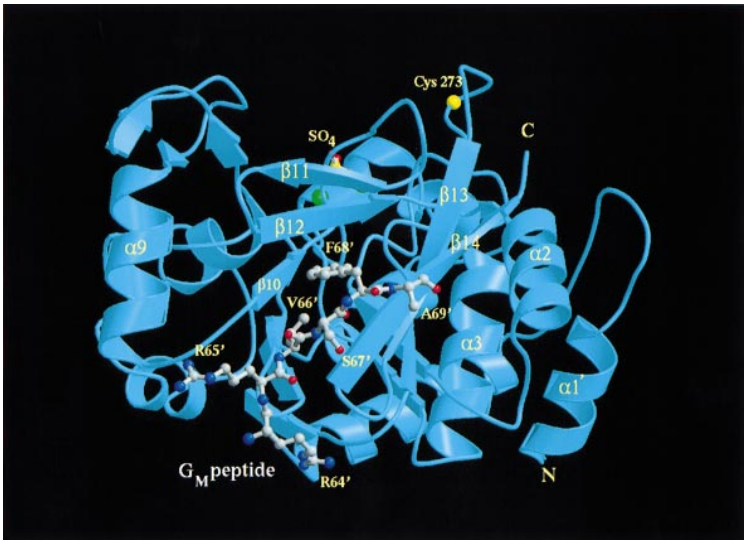
Cys 273
SO_4
C
β11
β13
β12
α9
F68'
β14
α2
β10
V66'
A69'
α3
R65'
S67'
α1'
$G_M$peptide
R64'
N

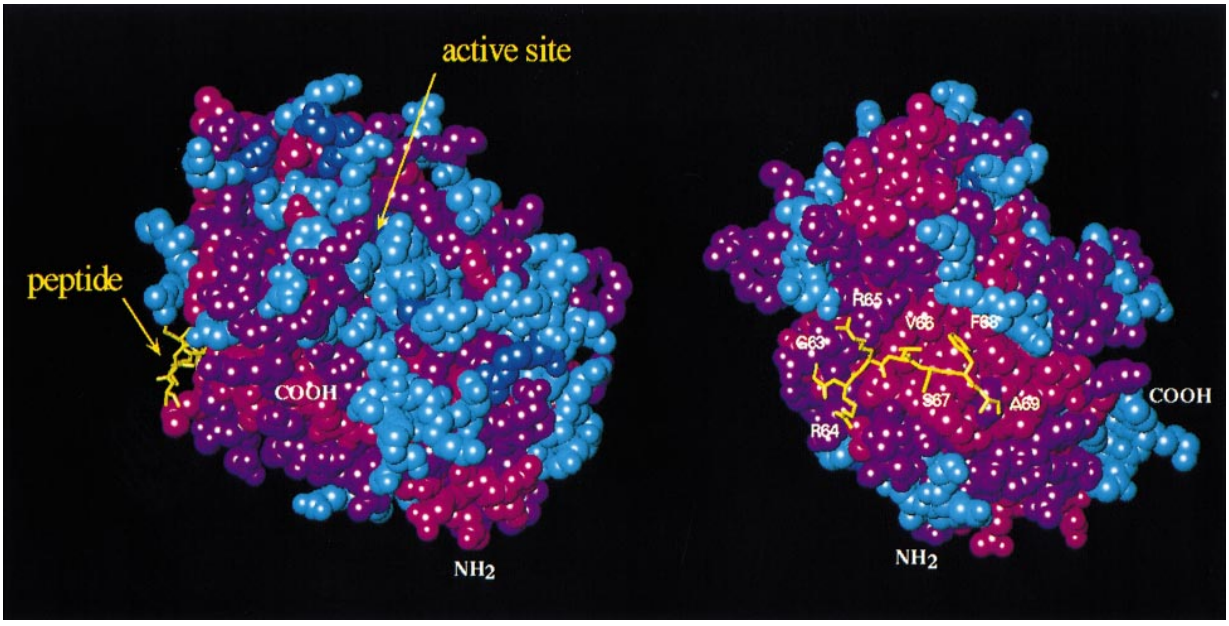
active site
peptide
COOH
NH_2
R65
V66
F68
G63
S67
A69
R64
COOH
NH_2

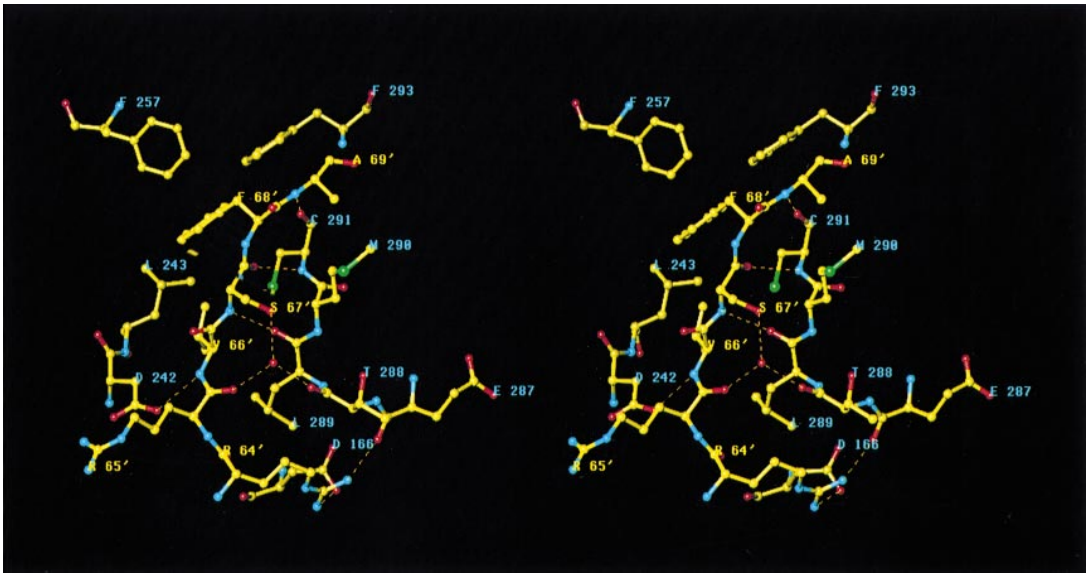
F 257
F 293
A 69'
F 68'
C 291
W 290
L 243
S 67'
V 66'
D 242
T 288
E 287
L 289
D 166
R 64'
R 65'

as well as the (R/K)(V/I)XF motif shared by PP1 regulatory subunits, the four residues N-terminal to this motif contain an abundance of basic residues. These residues may provide further favourable interactions with the negative electrostatic surface potential at the N-terminus of the $G_{M[63–75]}$ peptide-binding site of PP1c (Figure 2D).

Mutagenesis of the (R/K)(V/I)XF motif

The structural studies presented here suggest a dominant role for Val66′ and Phe68′ in stabilizing the interaction between $G_{M[63–75]}$ and PP1c, and this notion is reinforced further by the finding that other PP1 regulatory subunit sequences contain an (R/K)(V/I)XF motif yet share little overall sequence similarity. To test the hypothesis that Val66′ and Phe68′ are required for the interaction of $G_{M[63–75]}$ with PP1c and also that the KVKF sequence present within the $M_{110[M1–F38)}$ peptide is important in mediating its interaction with PP1c, we synthesized variations of the G_M and M_{110} peptides where the R/KVXF motif was disrupted. The two variants of the G_M peptide

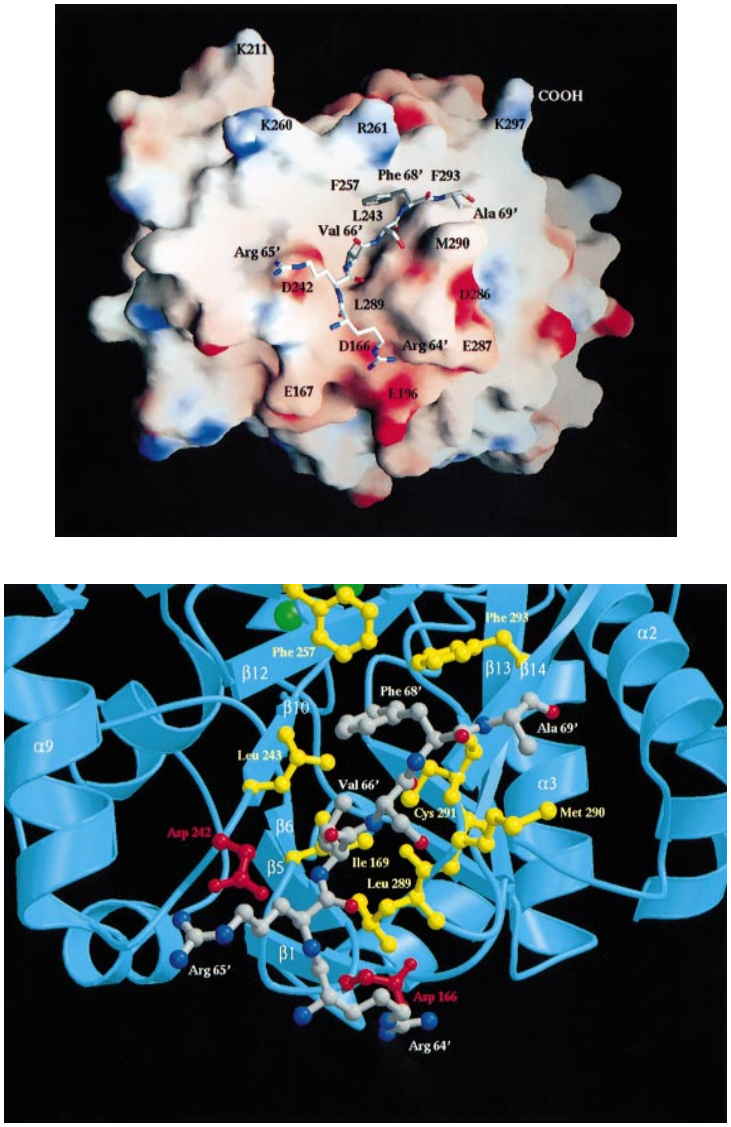

Fig. 2. Structure of PP1–$G_{M[63–75]}$ peptide complex. (**A**) A ribbons diagram of PP1c to indicate the position of the peptide-binding channel at the interface of the two β-sheets of the β-sandwich. The G_M peptide atoms are represented as ball-and-stick. The position of one of the metal ions at the catalytic site is indicated as a green sphere and the Cα of Cys273, whose side chain forms a covalent bond with the Mdha side chain of microcystin LR is shown as a yellow sphere (MOLSCRIPT, Kraulis, 1991). (**B**) Two perpendicular views of the surface of PP1c to show the hydrophobic peptide-binding channel. Residues 63′–69′ (GRRVSFA) of the $G_{M[63–75]}$ peptide are shown as sticks. The position of the sulfate ion bound at the catalytic site is indicated in one view and the N- and C-termini of PP1 are labelled. Drawn with TURBO-FRODO (Roussel and Cambillau, 1992). Pink: hydrophobic; purple: hydrophilic; cyan: acidic; blue: basic residues. (**C**) Stereo view of the residues 64′–69′ of the $G_{M[63–75]}$ peptide at the recognition site of PP1 to indicate polar interactions between peptide and protein and the formation of the β-sheet between Ser67′–Ala69′ and β14 of PP1. Drawn with TURBO-FRODO (Roussel and Cambillau, 1992). (**D**) Solvent-accessible surface and surface electrostatic potential of the PP1–$G_{M[63–75]}$ peptide complex calculated with PP1c coordinates alone and showing the peptide as a stick representation in the vicinity of the peptide-binding site. The protein surface is coloured according to electrostatic potential from red (most negative) to blue (most positive). The figure shows pronounced negative electrostatic potential in the region surrounding the N-terminus of the peptide-binding site that results from seven conserved acidic residues. Residues of PP1c in the vicinity of the peptide-binding site are labelled. The figure was created with GRASP (Nicholls and Honig, 1991). (**E**) Details of the structure of the peptide-binding site to show hydrophobic interactions between PP1c and Val66′, Phe68′ and Ala69′ of the $G_{M[63–75]}$ peptide (MOLSCRIPT, Kraulis, 1991).

Table II. PP1–peptide interactions

	Peptide atom	Protein atom	Water molecule	Distance (Å)
Polar interactions				
Molecule 1	Arg65′ O		7W	3.2
	Val66′ N	Asp242 OD2[a]		3.0
	Ser67′ N	Leu289 O		3.3
	Ser67′ OG		7W	2.7
	Ser67′ O	Cys291 N[b]		3.2
	Ala69′ N	Cys291 O[b]		2.8
Molecule 2	Arg64′ NH1	Glu287 O[a]		2.6
	Arg65′ O		7W	2.8
	Val66′ N	Asp242 OD2[a]		3.2
	Ser67′ N	Leu289 O[b]		3.1
	Ser67′ OG		7W	2.6
	Ser67′ O	Cys291 N[b]		3.0
	Ala69′ N	Cys291 O[b]		3.3
	Peptide residues	**Protein residues**		
Hydrophobic interactions	Val66′	Ile169[b], Leu243[b], Asp242[a], Leu289[b], Cys291[b]		
	Phe68′	Phe257[b], Cys291[b], Phe293[b]		
	Ala69′	Met290[a]		

[a]Highly conserved residues (Barton *et al.*, 1994).
[b]Invariant residues in all known PP1 sequences.

A

PP1-binding subunit	(R/K) (V/I)x F motif	Residues
G_M-subunit	S G G R **R V** S **F** A D N	61 - 71
G_L-subunit	K V K K **R V** S **F** A D N	57 - 67
G_L-related protein	Q A K K **R V** V **F** A D S	80 - 90
M_{110} subunit	R Q K T **K V** K **F** D D G	31 - 41
p53BP2	A H G M **R V** K **F** N P L	794 - 804
inhibitor-1	N S P R **K I** Q **F** T V P	5 - 15
DARPP32	K D R K **K I** Q **F** S V P	4 - 14
NIPP-1	R K N S **R V** T **F** S E D	196 - 206
splicing factor PSF	G R Q L **R V** R **F** A T H	12 - 22

B

protein	Putative PP1-binding motif	residues
GAC1	S P E **K** N **V** R **F** A I E	66-76
PIG2	S S G **K** S **V** R **F** A A H	50-60
GIP2	I R S **K** S **V** H **F** D Q A	217-227
YIL045W	Q R S **K** S **V** H **F** D R V	193-203
YIL045W	V F V **K** N **I** Y **F** S N A	412-422
REG1	T K N **R H I** H **F** N D R	461-471
REG2	P R E **R H I** K **F** N D N	164-174
SCD5	F K S **K K V** R **F** S E H	270-280
GIP1	W N L **K** F **I** P **F** N N L	180-190
GIP1	K K K **R** C **V** N **F** R N K	441-451

Fig. 3. Sequence alignment of PP1 regulatory subunits in the vicinity of the (R/K)(V/I)XF motif. (**A**) Mammalian PP1-binding subunits. G_M (Tang *et al.*, 1991); G_L (Doherty *et al.*, 1995); G_L-related protein (Doherty *et al.*, 1996); p53BP2 (Helps *et al.*, 1995); NIPP-1 (Van Eynde *et al.*, 1995); splicing factor PSF (Hirano *et al.*, 1996); M_{110} subunit (Chen *et al.*, 1994); inhibitor-1 (Aitken *et al.*, 1982); DARPP-32 (Williams *et al.*, 1986). (**B**) PP1-binding proteins in *S.cerevisiae*. GAC1 (Francois *et al.*, 1992); PIG2 (P.J.Roach, personal communication); GIP1, GIP2, YIL045W (Tu *et al.*, 1996); REG1, REG2 (Tu and Carlson, 1995; Frederick and Tatchell, 1996); SCD5 (Nelson *et al.*, 1996; Tu *et al.*, 1996). The region similar to the RRVSFA sequence of G_M which interacts with PP1c is boxed.

were Val66′ and Phe68′ to Ala substitutions. In order to disrupt the (R/K)(V/I)XF present within the M_{110} peptide, a peptide corresponding to residues Met1–Lys35 was synthesized which no longer contains the sequence VKF of the VXF motif, which is present at residues 36–38.

The results for the $M_{110[1–38]}$ and $M_{110[1–35]}$ peptides (Figures 5 and 6A) are unequivocal. Whereas $M_{110[1–38]}$ stimulates the myosin light chain phosphatase activity of PP1c with a half-maximal effect at 10 nM reaching maximal (3-fold) activation at a peptide concentration of 1 μM as reported previously (Johnson *et al.*, 1996), the $M_{110[1–35]}$ peptide was at least 10^4-fold less effective at activating PP1c (Figure 5). Unlike $M_{110[1–38]}$, the $M_{110[1–35]}$ peptide was also unable to activate the phosphorylase phosphatase activity of liver PP1–G_L (Figure 6A). This latter result suggests two conclusions. First, that although $M_{110[1–38]}$ is able to bind to PP1c and disrupt the interactions between PP1c and the G_L subunit, hence reversing the inhibitory effects of G_L on the ability of PP1c to dephosphorylate phosphorylase, loss of the VKF sequence in the $M_{110[1–38]}$ peptide abolishes the ability of the peptide to disrupt this interaction. Secondly, the recognition site on PP1c for the VKF sequence of the $M_{110[1–38]}$ peptide must overlap with the binding site for the G_L subunit, suggesting that the VKF sequence binds to the same site as the VSF sequence of G_L that is identical with that present in the $G_{M[63–75]}$ peptide. Similar conclusions may be reached from the results obtained from disrupting the VXF motif

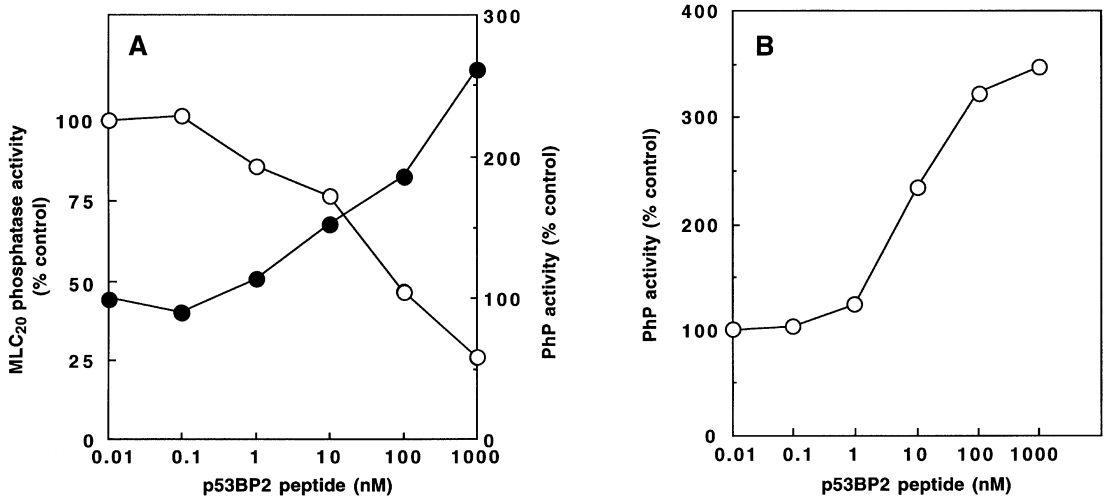

Fig. 4. Disruption of the interactions between PP1c and the G_L and M_{110} subunits by a synthetic peptide from p53BP2. (**A**) PP1M from chicken gizzard smooth muscle (Alessi *et al.*, 1992) was diluted and incubated for 15 min at 30°C with the peptide GKRTNLRKTGSERIAHGMRVK-FNPLALLLDSC, corresponding to the sequence in p53BP2 that contains the RVXF motif. Reactions were started with either ^{32}P-labelled MLC_{20} or glycogen phosphorylase, and the MLC_{20} phosphatase (○) and phosphorylase phosphatase (PhP, ●) activities were determined. The results are expressed as a percentage of the activity determined in control incubations where the p53BP2 peptide was omitted (100%). Similar results were obtained in three separate experiments. (**B**) Same as (A), except that the peptide was incubated with diluted hepatic glycogen particles containing PP1–G_L before measuring the PhP activity. Similar results were obtained in three separate experiments.

within the $G_{M[63–75]}$ peptide (Figure 6B). Substitution of Phe68′ for Ala completely abolishes the ability of $G_{M[63–75]}$ to disrupt the PP1–G_L complex, whereas replacement of Val66′ with Ala reduced the effectiveness of the disruption 100-fold.

Regulation of the PP1–G_M complex by phosphorylation of Ser67′

The sequence of G_M surrounding Ser67′ (RRVSFA) conforms to a consensus PKA recognition sequence, and phosphorylation of Ser67′ by PKA promotes dissociation of both G_M and $G_{M[63–75]}$ from PP1c *in vitro* and *in vivo*. This releases PP1c from glycogen particles preventing it from inactivating glycogen phosphorylase and activating glycogen synthase (reviewed in Hubbard and Cohen, 1993). Interestingly, Ser67′ corresponds to residue X of the VXF motif, and the β-strand conformation of the peptide RRVSFA bound to PP1c is similar to the pseudo-substrate sequence of PKI (residues 18–23) which binds to the catalytic site of PKA (Knighton *et al.*, 1991). Although the side chain of Ser67′ is exposed within the PP1c–peptide complex, overall the G_M peptide is buried, and it is unlikely that Ser67′ would be a substrate for PKA when the peptide is bound to PP1c. This would suggest that PKA phosphorylates Ser67′ when G_M is not associated with PP1c and that this phosphorylation prevents the re-association of PP1c with G_M. Since phosphorylation of Ser67′ promotes the dissociation of the PP1–G_M complex both *in vivo* and *in vitro*, it is most likely that PKA phosphorylates Ser67′ of G_M by competing with PP1c for the RRVSFA sequence. This is consistent with the notion that the PP1–G_M complex exists in dynamic equilibrium with free PP1c and G_M subunits and that phosphorylation occurs on the regulatory subunit during transient dissociation from PP1c. In the PP1c–peptide complex, the side chain of Ser67′ adopts the most favourable rotamer conformation. Analysis of the PP1c–peptide complex structure suggests that incorporation of a phosphate group onto the side chain of Ser67′ with the same side-chain rotamer conformation would cause steric hindrance between the peptide and Met290 of PP1 and also introduce a phosphate group into a region of negative charge at the PP1c surface (Figure 2C and D). This may explain how phosphorylation of Ser67′ prevents peptide association with PP1c, although it should be noted that rotation of the side chain of Ser67′ would relieve this steric clash.

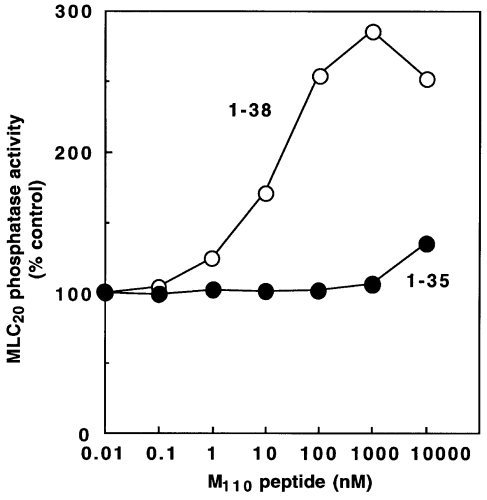

Fig. 5. Effect of $M_{110[M1–F38]}$ and $M_{110[M1–K35]}$ on the PP1c-catalysed dephosphorylation of MLC_{20}. $M_{110[M1–F38]}$ (1–38, ○) or $M_{110[M1–K35]}$ (1–35, ●) were incubated with PP1c for 15 min at 30°C and reactions started with the ^{32}P-labelled MLC_{20} substrate. The results are expressed as a percentage of the activity determined in control incubations where the M_{110} peptides were omitted (100%). Similar results were obtained in three separate experiments.

A similar mechanism of control may also operate for other PP1 regulatory subunits. For example, NIPP-1, a nuclear inhibitor of PP1, inhibits PP1 with an inhibitory constant of 1 pM (Beullens *et al.*, 1992). Phosphorylation

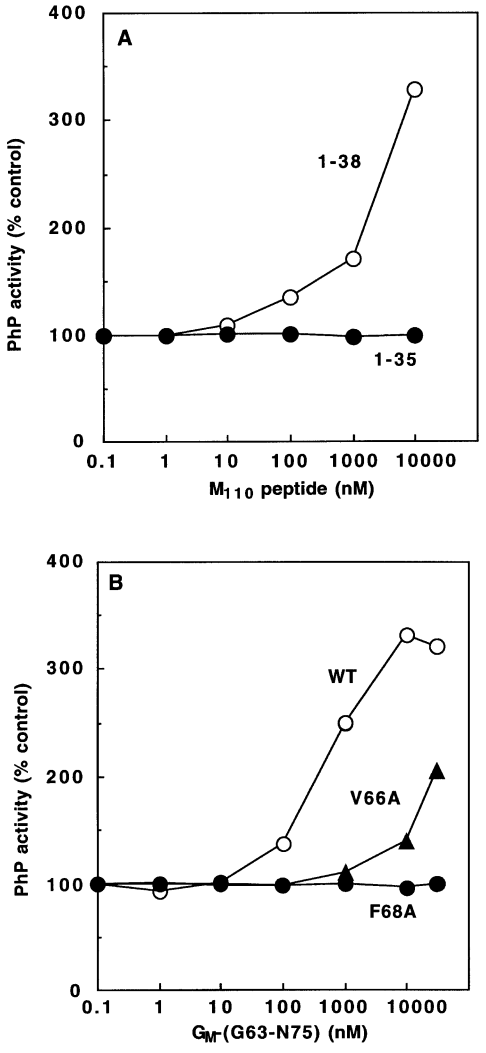

Fig. 6. Effect of synthetic peptides derived from the M_{110} and G_M subunits on the phosphorylase phosphatase activity of PP1–G_L. (**A**) Hepatic glycogen protein particles containing PP1–G_L were diluted and incubated for 15 min at 30°C with the indicated concentrations of either $M_{110[M1–F38]}$ (○) or $M_{110[M1–K35]}$ (●) and the phosphatase reactions were initiated by addition of ^{32}P-labelled glycogen phosphorylase. The results are expressed as a percentage of the activity determined in control incubations where the M_{110} peptides were omitted. Similar results were obtained in three separate experiments. (**B**) The experiment was carried out as in (A), except that the peptide $G_{M[G63–N75]}$ ('wild type', WT) and variants in which either Val66 (V66A) (▲) or Phe68 (F68A) (●) were changed to Ala were used instead of the M_{110} peptides. Similar results were obtained in three separate experiments.

of NIPP-1 by PKA and/or casein kinase 2 *in vitro* abolishes this inhibition (Beullens *et al.*, 1993; Van Eynde *et al.*, 1994). Although the sites of phosphorylation on NIPP-1 that mediate these effects are not yet fully characterized, it is known that these sites occur within the central ~120 residues of NIPP-1 that incorporate the (R/K)(V/I)XF motif (Van Eynde *et al.*, 1995). Interestingly, a consensus phosphorylation site for PKA (RKNS) occurs immediately N-terminal to this motif, whereas one casein kinase 2 consensus phosphorylation site occurs between the Val and Phe of the motif and another occurs immediately C-terminal to the Phe residue (TFSEDDE) (Van Eynde *et al.*, 1995) (Figure 3A). It is possible that PKA, casein kinase 2 or other kinases with similar specificity, release PP1c from inhibition by NIPP-1 by phosphorylating NIPP-1 at sites that block its interaction with the (R/K)(V/I)XF motif recognition site on PP1c.

Prediction of PP1 recognition motifs in yeast PP1-binding proteins

The residues in mammalian PP1c that interact with the sequence RRVSFA are conserved in *Saccharomyces cerevisiae* PP1, suggesting that the proteins in *S.cerevisiae* known to interact with PP1 (reviewed by Stark, 1996) probably bind to a similar hydrophobic groove on the surface of the enzyme. Examination of their amino acid sequences revealed that a number of PP1-binding proteins in *S.cerevisiae* contained putative PP1-binding motifs that were similar to those present in mammalian PP1-binding proteins (Figure 3A and B). The *S.cerevisiae* PP1-binding proteins not only contain a (V/I)XF motif, but also a basic residue equivalent to Arg64′ of G_M, the residue that contacts Asp166, Leu289 and the main-chain carbonyl of Glu287 of PP1c. Several of the *S.cerevisiae* proteins also contain a further basic residue (His or Lys) at the position equivalent to Arg65′ of G_M. Another striking feature of the putative PP1-binding sequences in *S.cerevisiae* is the presence of a basic amino acid between the Val/Ile and Phe residues, as is also found in two mammalian PP1 regulatory subunits, the M_{110} subunit and the p53BP2 (Figure 3A).

The *S.cerevisae* proteins GAC1 and PIG2 show some homology to residues 140–230 of mammalian G_M, and there is genetic and biochemical evidence that they may function to regulate glycogen metabolism in budding yeast (Francois *et al.*, 1992; P.J.Roach, personal communication). GIP2 also shares sequence similarity with residues 140–230 of mammalian G_M, while YIL045W is an open reading frame in the *S.cerevisiae* genome whose predicted amino acid sequence shows 41% sequence identity to GIP2. YIL045W contains two potential PP1-binding motifs. REG1 and REG2 are PP1-binding proteins that play a role in cell growth and, in the case of REG1, glucose repression (Tu and Carlson, 1995; Frederick and Tatchell, 1996; Tu *et al.*, 1996). GIP1, which also contains two potential PP1-binding motifs, is expressed specifically during meiosis, affects the transcription of late meiotic genes and is essential for sporulation (Tu and Carlson, 1995). SCD5 is a PP1-interacting protein (Tu *et al.*, 1996) that was first isolated as a multicopy suppressor of the inviability of clathrin heavy chain-deficient yeast (Nelson *et al.*, 1996). Site-directed mutagenesis of these putative PP1-binding motifs will be needed to establish whether they are critical for binding to PP1c.

Concluding remarks

The importance of short peptide sequences of 4–6 residues in mediating crucial protein–protein interactions and in determining the subcellular localization of proteins has become increasingly apparent in recent years. Such sequences include the pYXXM motifs that mediate interactions with SH2 domains (Zhou *et al.*, 1995), the E(S/T)XV motif that mediates interactions with the PDZ domain (Doyle *et al.*, 1996), the KDEL motif that is critical for the targeting of proteins to the lumen of the endoplasmic reticulum (Pelham, 1992) and nuclear export and import sequences (Dingwall and Laskey, 1991). The

short linear sequence LFG was shown recently to be a critical determinant of the interaction between the $p27^{Kip1}$ cyclin-dependent kinase inhibitor and the cyclin A–CDK2 complex (Russo *et al.*, 1996). A similar motif, that is present within the proteins p21 and p107, is essential for the inhibition of cyclin–CDK by p21 and for the tight binding of the substrate p107 to cyclin–CDK (Zhu *et al.*, 1995). The ability of proteins to recognize relatively short linear sequence motifs with a high degree of specificity provides a means whereby novel protein–protein interactions and macromolecular assemblies may evolve relatively rapidly and simply with subsequent generation of specific signalling responses.

The findings presented here demonstrate that another short peptide sequence, the (R/K)(V/I)XF motif, is critical for PP1c to interact with its regulatory subunits. Interestingly, the extension of the PP1c β-sheet by the $G_{M[63–75]}$ peptide is similar to the interactions of the PTB and PDZ domains with their cognate peptide ligands (Zhou *et al.*, 1995; Doyle *et al.*, 1996). PP1c (when complexed to its targeting subunits) plays key roles in the control of many cellular processes, and it is reasonable to predict that >100 PP1-binding proteins may exist in mammalian cells. Protein sequence database searching has revealed that the (R/K)(V/I)XF motif is found in 10% of proteins. Thus if ~100 PP1-binding proteins occur in mammalian cells, only 1% of proteins with the (R/K)(V/I)XF motif will be PP1-binding proteins. The reasons why only a few proteins with the (R/K)(V/I)XF motif bind to PP1 are numerous. For example, not every residue may be tolerated at position X or immediately N-terminal or C-terminal to this motif. This study has shown that phosphoserine is not tolerated at position X and it is therefore likely that Asp or Glu will not be tolerated either. The structure of the PP1–$G_{M[63–75]}$ complex suggests that large hydrophobic residues will also be excluded from position X. Moreover, the Val (or Ile) and Phe residues in many (R/K)(V/I)XF motifs will be buried in the hydrophobic core of the protein and hence be unable to interact with PP1, since this motif is predicted to form an amphipathic β-strand conformation. Thirdly, many of the (R/K)(V/I)XF motifs will be in extracellular proteins or extracellular domains of transmembrane proteins and hence be unable to bind to PP1. Particular features of the tertiary structure of PP1-binding proteins may allow exposure of this motif on the surface to enable interaction with PP1. Finally, there is evidence that a second PP1-binding site exists on the G_M and M_{110} subunits (Johnson *et al.*, 1996) and the high affinity interaction of PP1c with protein inhibitor-1 is generated by the binding of PP1c to two low affinity sites (Desdouits *et al.*, 1995), one of which is the KIQF sequence belonging to the (R/K)(V/I)XF motif.

The question of how regulatory subunits modulate the substrate specificity of PP1c requires the co-crystallization of PP1c with a diverse array of regulatory subunits and substrates and is beyond the scope of this study. However, two models to account for this property of regulatory subunits are that these subunits either alter the conformation of PP1c or simply target PP1 to its substrates. Both mechanisms may operate *in vivo* depending on the regulatory subunits and substrates. For example, evidence for the former model has been reported recently for the enhancement of myosin dephosphorylation by a complex of PP1c and the M_{110} subunit (Johnson *et al.*, 1996, 1997), whereas the enhancement of the dephosphorylation of glycogen phosphorylase and glycogen synthase by the PP1–G_M complex is more consistent with the second model (Hubbard and Cohen, 1989).

The identification of the (R/K)(V/I)XF motif also suggests a new approach for determining the physiological roles of PP1 targeting subunits whose functions are unknown. Thus mutation of the (R/K)(V/I)XF motif should disrupt the interaction of many targeting subunits with PP1c without affecting their binding to the target locus. Expression of these mutated proteins under an inducible promoter should lead to displacement of the normal targeting subunit (complexed to PP1c) from its target locus, without disrupting the functions of any other PP1c–targeting subunit complex. Finally, the structural information reported here should also facilitate the rational design of drugs that act by disrupting PP1–targeting subunit interactions.

Materials and methods

Crystallization and data collection

The catalytic subunit of PP1γ1 was expressed in *Escherichia coli* and purified as described previously (Alessi *et al.*, 1993; Barford and Keller, 1994). The $G_{M[G63–N75]}$ peptide, variants of this peptide in which Val66′ or Phe68′ were changed to Phe, the peptides $M_{110[1–38]}$ and $M_{110[1–35]}$ and a 32 residue peptide corresponding to residues 780–811 of p53BP2 were synthesized on an Applied Biosystems 430A peptide synthesizer and purified by chromatography on a C18 column (Johnson *et al.*, 1996) by Mr F.B.Caudwell at Dundee. A 3-fold molar excess of $G_{M[G63–N75]}$ was added to the protein solution (8 mg/ml), which had been dialysed previously against 10 mM Tris–HCl (pH 7.8), 0.3 M NaCl, 0.4 mM $MnCl_2$ and 2 mM dithiothreitol (DTT). The complex was crystallized at 20°C using the hanging drop vapour diffusion method, by mixing 2 μl of the protein–peptide solution and 2 μl of the precipitant solution containing 2.0 M ammonium sulfate, 2% (w/v) polyethylene glycol (PEG) 400, 100 mM HEPES (pH 7.5) and 2 mM DTT. These conditions are very much in contrast to the relatively low ionic strength conditions from which the monoclinic PP1c crystals grew (Barford and Keller, 1994; Egloff *et al.*, 1995). Crystals appeared after 3 months as a cluster. Individual crystals removed from the cluster had dimensions of ~25 μm×25 μm×5 μm. Unfortunately, the generation of these crystals was not reproducible. Crystals were frozen in a 100 K nitrogen gas stream and stored. Prior to freezing, crystals were incubated in a cryoprotectant solution consisting of an equilibration buffer; 2.0 M ammonium sulfate, 2% (w/v) PEG 400, 100 mM HEPES (pH 7.5) with increasing amounts of glycerol in steps of 7, 15, 22 and 30% (v/v).

A partial data set to 3.0 Å was collected on Beam Line PX 9.6, SRS, Daresbury, using a 30 cm diameter Mar Research image plate system. Data were processed and scaled using DENZO and SCALEPACK (Otwinowski, 1993). The crystal system is tetragonal with point group symmetry P422 and unit cell dimensions $a = b = 62.50$ Å, $c = 361.30$ Å. Systematic absences indicate a 2_1 screw axis along *b*. The Matthews coefficient was 2.38 $Å^3$ per Dalton, assuming two molecules per asymmetric unit. A second data set was collected on BL4 at the ESRF, Grenoble. Substantial radiation damage was observed during data collection requiring that three crystals were used in total. Data collected from four crystals at Daresbury and the ESRF were merged together in SCALEPACK. Details of the data collection and processing statistics are given in Table I.

Structure determination

The structure of the PP1–$G_{M[63–75]}$ peptide complex was solved by molecular replacement using as a model the protein atom coordinates of the 2.5 Å refined structure of the catalytic subunit of PP1γ1 determined by MAD methods (Egloff *et al.*, 1995). Rotation and translation function searches were performed with AMORE (Navaza, 1992). Using data between 8 and 3 Å resolution, the peak in the rotation search was 6.7 standard deviations (SD) above the mean. The translation search was best performed using data between 8 and 3.5 Å, giving a maximal peak

at 13.8 SD above the mean for the space group $P4_12_12$. After the first rigid body refinement performed in AMORE, the *R*-factor was 0.494 and the correlation factor 0.30.

Crystallographic refinement

The solution from molecular replacement was optimized by 20 cycles of rigid body refinement performed with X-PLOR version 3.1 (Brünger, 1992), using data between 8.0 and 3.0 Å resolution. After a round of conjugate gradient positional refinement and simulated annealing molecular dynamics to 2000 K, followed by 25 cycles of grouped *B*-factor refinement (two *B*-factor groups for each residue), the *R*-factor (respectively free-*R*) was 0.295 (0.367). Initally, non-crystallographic symmetry restraints (200 kcal/mol) were applied during refinement, that were removed during the final stages of refinement. Fourier difference maps (F_o–F_c) and ($3F_o$–$2F_c$) revealed the presence of three strong peaks (over three times the σ level of the map) at the catalytic site of PP1c. From the previously refined PP1c structure, we identified two as manganese and iron ions. The third one, occupying the position of the tungstate ion in the PP1c–WO_4 complex, was identified as sulfate. The initial difference Fourier maps also revealed strong electron density near the N-terminus of β14. The maps were improved by applying non-crystallographic symmetry 2-fold averaging using PHASES (Furey and Swaminathan, 1990). As shown in Figure 1A, residues Val66′, Ser67′ and Phe68′ of the $G_{M[63–75]}$ peptide were identified in the averaged map. These three residues, as well as the one sulfate and two metal ions, were built into each molecule using the program TURBO-FRODO (Roussel and Cambillau, 1992). Refinement of this structure was performed by repeated rounds of manual rebuilding followed by conjugate gradient positional refinement and grouped *B*-factor refinement using X-PLOR. The final model contains protein residues Lys6–Ala299 and peptide residues Arg65′–Ala69′ in molecule 1, and protein residues Asn8–Lys297 and peptide residues Gly63′–Ala69′ in molecule 2. A few well defined water molecules were also observed in both initial ($3F_o$–$2F_c$) and (F_o–F_c) electron density maps. Eventually, 14 water molecules that were above 3σ in the (F_o–F_c) difference map, within hydrogen bonding distance of the PP1–peptide complex or another solvent molecule and present in both molecules, were included in the model. The crystallographic and refinement data are summarized in Table I. Representative electron density from the peptide before and after refinement is shown in Figure 1A and B, respectively. Solvent-accessible surface areas were calculated using the method of Lee and Richards (1971).

Purification and assay of PP1

PP1c was isolated from the rabbit skeletal muscle PP1–G_M complex as described previously (Johnson *et al.*, 1996). Glycogen particles isolated from rat liver (Schelling *et al.*, 1988) served as the source of PP1–G_L. The dephosphorylation of glycogen phosphorylase (10 μM) and the isolated MLC_{20} of smooth muscle myosin (1 μM) by PP1c was carried out as described previously (Cohen *et al.*, 1988; Alessi *et al.*, 1992).

Acknowledgements

We thank Dr E.Mitchell, BL4, ESRF Grenoble and the staff at PX9.6, Daresbury for assistance, Mr F.B.Caudwell for peptide synthesis and Dr N.Helps for valuable discussions. We acknowledge the award of an EMBO Long Term Fellowship (ALTF 748-1994) to M.-P.E. and an MRC postgraduate studentship to D.F.J. This work was supported by grants from the UK Medical Research Council (D.B., P.C. and P.T.W.C.) and the Royal Society of London.

References

Aitken,A. and Cohen,P. (1982) Isolation and characterisation of active fragments of protein phosphatase inhibitor-1 from rabbit skeletal muscle. *FEBS Lett.*, **147**, 54–58.

Aitken,A., Bilham,T. and Cohen,P. (1982) Complete primary structure of protein phosphatase 1 inhibitor 1 from rabbit skeletal muscle. *Eur. J. Biochem.*, **126**, 235–246.

Alessi,D.R., McDougall,L.K., Sola,M.M., Ikebe,M. and Cohen,P. (1992) The control of protein phosphatase-1 by targeting subunits. *Eur. J. Biochem.*, **210**, 1023–1035.

Alessi,D.R., Street,A.J., Cohen,P. and Cohen,P.T.W. (1993) Inhibitor-2 functions like a chaperone to fold three expressed isoforms of mammalian protein phophatase-1 into a conformation with the specificity and regulatory properties of the native enzyme. *Eur. J. Biochem.*, **213**, 1055–1066.

Barford,D. and Keller,J.C. (1994) Co-crystallization of the catalytic subunit of the serine/threonine specific protein phosphatase 1 from human in complex with microcystin LR. *J. Mol. Biol.*, **235**, 763–766.

Barton,G.J., Cohen,P.T.W. and Barford,D. (1994) Conservation analysis and structure prediction of the protein serine/threonine phosphatases. *Eur. J. Biochem.*, **220**, 225–237.

Brünger,A.T. (1992) *X-PLOR: Version 3.1; A System for Protein Crystallography and NMR*. Yale University Press, New Haven, CT.

Beullens,M., Van Eynde,A., Stalmans,W. and Bollen,M. (1992) The isolation of novel inhibitory polypeptides of protein phosphatase 1 from bovine thymus nuclei. *J. Biol. Chem.*, **267**, 16538–16544.

Beullens,M., Van Eynde,A., Bollen,M. and Stalmans,W. (1993) Inactivation of nuclear inhibitory polypeptides of protein phosphatase-1 (NIPP-1) by protein kinase A. *J. Biol. Chem.*, **268**, 13172–13177.

Beullens,M., Stalmans,W. and Bollen,M. (1996) Characterisation of a ribosomal inhibitory polypeptide of protein phosphatase-1 from rat liver. *Eur. J. Biochem.*, **239**, 183–189.

Cohen,P. (1989) The structure and regulation of protein phosphatases. *Annu. Rev. Biochem.*, **58**, 453–508.

Cohen,P. (1992) Signal integration at the level of protein kinases, protein phosphatases and their substrates. *Trends Biochem. Sci.*, **17**, 408–413.

Cohen,P., Alemany,S., Hemmings,B.A., Resink,T.J., Stralfors,P. and Tung,H.Y.L. (1988) Protein phosphatase 1 and protein phosphatase 2A from rabbit skeletal muscle. *Methods Enzymol.*, **159**, 390–408.

Desdouits,F. *et al.* (1995) Mechanism of inhibition of protein phosphatase 1 by DARPP-32: studies with recombinant DARPP-32 and synthetic peptides. *Biochem. Biophys. Res. Commun.*, **206**, 653–658.

Derrick,J.P. and Wigley,D.B. (1992) Crystal structure of a streptococcal protein G domain bound to an Fab fragment. *Nature*, **359**, 752–754.

Dingwall,C. and Laskey,R.A. (1991) Nuclear targeting sequences—a consensus? *Trends Biochem. Sci.*, **16**, 478–481.

Doherty,M.J., Moorhead,G., Morrice,N., Cohen,P. and Cohen,P.T.W. (1995) Amino acid sequence and expression of the hepatic glycogen-binding G_L-subunit of PP1. *FEBS Lett.*, **375**, 294–298.

Doherty,M.J., Young,P.R. and Cohen,P.T.W. (1996) Amino acid sequence of a novel protein phosphatase 1 binding protein (R5) which is related to the liver and muscle specific glycogen binding subunits of protein phosphatase 1. *FEBS Lett.*, **399**, 339–343.

Doyle,D.A., Lee,A., Lewis,J., Kim,E., Sheng,M. and MacKinnon,R. (1996) Crystal structures of a complexed and peptide-free membrane protein-binding domain: molecular basis of peptide recognition by PDZ. *Cell*, **85**, 1067–1076.

Durfee,T., Becherer,K., Chen,P.-L., Yeh,S.-H., Yang,Y., Kilburn,A.E., Lee,W.-H. and Elledge,S.J. (1993) The retinoblastoma protein associates with the protein phosphatase type 1 catalytic subunit. *Genes Dev.*, **7**, 555–569.

Egloff,M.-P., Cohen,P.T.W., Reinemer,P. and Barford,D. (1995) Crystal structure of the catalytic subunit of human protein phosphatase 1 and its complex with tungstate. *J. Mol. Biol.*, **254**, 942–959.

Endo,S., Zhou,X., Connor,J., Wang,B. and Shenolikar,S. (1996) Multiple structural elements define the specificity of recombinant human inhibitor-1 as a protein phosphatase-1 inhibitor. *Biochemistry*, **35**, 5220–5228.

Faux,M.C. and Scott,J.D. (1996) More on target with protein phosphorylation: conferring specificity by location. *Trends Biochem. Sci.*, **21**, 312–315.

Francois,J.M., Thompson-Jaeger,S., Skroch,J., Zellenka,U., Spevak,W. and Tatchell,K. (1992) GAC1 may encode a regulatory subunit for protein phosphatase type 1 in *Saccharoymes cerevisiae*. *EMBO J.*, **11**, 87–96.

Frederick,D.L. and Tatchell,K. (1996) The REG2 gene of *Saccharomyces cerevisiae* encodes a type 1 protein phosphatase-binding protein that functions with Reg1p and the Snf1 protein kinase to regulate growth. *Mol. Cell Biol.*, **16**, 2922–2931.

Furey,W. and Swaminathan,S. (1990) PHASES: a program package for the processing and analysis of diffraction data from macromolecules. *Am. Crystallogr. Assoc. Meeting Summary*, **18**, 73.

Goldberg,J., Huang,H., Kwon,Y., Greengard,P., Nairn,A.C. and Kuriyan,J. (1995) Three dimensional structure of the catalytic subunit of protein serine/threonine phosphatase-1. *Nature*, **376**, 745–753.

Griffith,J.P. *et al.* (1995) X-ray structure of calcineurin inhibited by the immunophilin–immunosuppressant FKBP12–FK506 complex. *Cell*, **82**, 507–522.

Helps,N., Barker,H., Elledge,S.J. and Cohen,P.T.W. (1995) Protein phosphatase 1 interacts with p53BP2, a protein which binds to the tumour supressor p53. *FEBS Lett.*, **377**, 295–300.

Hemmings,H.C.,Jr, Nairn,A.C., Elliot,J.R. and Greengard,P. (1990) Synthetic peptide analogs of DARPP-32, an inhibitor of protein phosphatase-1. *J. Biol. Chem*., **265**, 20369–20376.

Hirano,K., Ito,M. and Hartshorne,D.J. (1995) Interaction of the ribosomal protein, L5, with protein phosphatase type 1. *J. Biol. Chem*., **270**, 19786–19790.

Hirano,K., Erdodi,F., Patton,J.G. and Hartshorne,D.J. (1996) Interaction of protein phosphatase type 1 with a splicing factor. *FEBS Lett*., **389**, 191–194.

Hubbard,M.J. and Cohen,P. (1989) Regulation of protein phosphatase-1G from rabbit skeletal muscle; 2. Catalytic subunit translocation is a mechanism for reversible inhibition towards glycogen bound substrates. *Eur. J. Biochem*., **186**, 711–716.

Hubbard,M.J. and Cohen,P. (1993) On target with a new mechanism for the regulation of protein phosphorylation. *Trends Biochem. Sci*., **18**, 172–177.

Hunter,T. (1995) Protein kinases and phosphatases: the yin and yang of protein phosphorylation and signalling. *Cell*, **80**, 225–236.

Jagiello,I., Beullens,M., Stalmans,W. and Bollen,M. (1995) Subunit structure and regulation of protein phosphatase-1 in rat liver nuclei. *J. Biol. Chem*., **270**, 17257–17263.

Johnson,D.F., Moorhead,G., Caudwell,F.B., Cohen,P., Chen,Y.-H., Chen,M.-X. and Cohen,P.T.W. (1996) Identification of protein phosphatase-1-binding domains on the glycogen and myofibrillar targeting subunits. *Eur. J. Biochem.*, **239**, 317–325.

Johnson,D., Cohen,P., Chen,M.-X., Chen,Y.-H. and Cohen,P.T.W. (1997) Identification of the regions of the M_{110} subunit of protein phosphatase 1M that interacts with the M_{21} subunit and with myosin. *Eur. J. Biochem*., in press.

Kissinger,C.R. *et al*. (1995) Crystal structure of human calcineurin and the human FKBP12–FK506–calcineurin complex. *Nature*, **378**, 641–644.

Knighton,D.R., Zheng,J., Ten Eyck,L.F., Xuong,N.-H., Taylor,S.S. and Sowadski,J.M. (1991) Structure of a peptide inhibitor bound to the catalytic subunit of cyclic adenosine monophosphate-dependent protein kinase. *Science*, **253**, 414–420.

Kraulis,P.J. (1991) MOLSCRIPT: a program to produce both detailed and schematic plots of protein structures. *J. Appl. Crystallogr*., **24**, 946–950.

Lee,B. and Richards,F.M. (1971) The interpretation of protein structures: estimation of static accessibilty. *J. Mol. Biol.*, **55**, 379–400.

Mermoud,J.E., Cohen,P. and Lamond,A.I. (1992) Ser/Thr-specific protein phosphatases are required for both catalytic steps of pre-mRNA splicing. *Nucleic Acid Res*., **20**, 5263–5269.

Moorhead,G., MacKintosh,W., Morrice,N., Gallagher,T. and MacKintosh,C. (1994) Purification of type 1 protein (serine/threonine) phosphatases by microcystin–Sepharose affinity chromatography. *FEBS Lett*., **356**, 46–50.

Moorhead,G., MacKintosh,C., Morrice,N. and Cohen,P. (1995) Purification of the hepatic glycogen-associated form of protein phosphatase-1 by microcystin–Sepharose affinity chromatography. *FEBS Lett*., **362**, 101–105.

Nassar,N., Horn,G., Herrman,C., Scherer,A., McCormick,F. and Wittinghofer,A. (1995) The 2.2 Å crystal structure of the ras-binding domain of the serine/threonine kinase c-Raf1 in complex with Rap1A and a GTP analogue. *Nature*, **375**, 554–560.

Naumovski,L. and Cleary,M.L. (1996) The p53-binding protein p53BP2 also interacts with Bcl2 and impedes cell cycle progression at G2/M. *Mol. Cell. Biol*., **16**, 3884–3892.

Navaza,J. (1992) AMoRe: a new package for molecular replacement. In Dodson,E.J., Grower,S. and Wolf,W. (eds), *Proceedings of the CCP4 Study Weekend*. SERC, Daresbury Laboratory, Warrington, UK, pp. 87–91.

Nelson,K.K., Holmes,M. and Lemmon,S.K. (1996) SCD5, a suppressor of clathrin deficiency encodes a novel protein with a late secretory function in yeast. *Mol. Biol. Cell*, **7**, 245–260.

Nicholls,A. and Honig,B. (1991) A rapid finite difference algorithm, utilising successive over relaxation to solve the Poisson–Boltzmann equation. *J. Comput. Chem*., **12**, 435–445.

Otwinowski,Z. (1993) DENZO. In Sawyer,L., Isaacs,N. and Bailey,S. (eds), *Data Collection and Processing*. SERC Daresbury Laboratory, Warrington, UK, pp. 56–62.

Pelham,H.R. (1992) The Florey Lecture, 1992. The secretion of proteins by cells. *Proc. R. Soc. Lond. Ser. B*, **B250**, 1–10.

Roussel,A. and Cambillau,C. (1992) *TURBO-FRODO*. Biographics, LCCMB, Marseille, France.

Russo,A.A., Jeffry,P.D., Patten,A.K., Massague,J. and Pavletich,N.P. (1996) Crystal structure of the $p27^{Kip1}$ cyclin-dependent-kinase inhibitor bound to the cyclin A–Cdk2 complex. *Nature*, **382**, 325–331.

Schelling,D.L., Leader,D.P., Zammit,V.A. and Cohen,P. (1988) Distinct type-1 protein phosphatases are associated with hepatic glycogen and microsomes. *Biochim. Biophys. Acta*, **927**, 221–231.

Shenolikar,S. (1994) Protein serine/threonine phosphatases—new avenues for cell regulation. *Annu. Rev. Cell Biol.*, **10**, 56–86.

Stark,M. (1996) Yeast protein serine/threonine phosphatases: multiple roles and diverse forms of regulation. *Yeast*, **12**, 1647–1675.

Stralfors,P., Hiraga,A. and Cohen,P. (1985) The protein phosphatases involved in cellular regulation. Purification and characterisation of the glycogen-bound form of protein phosphatase 1 from skeletal muscle. *Eur. J. Biochem*., **149**, 295–303.

Tang,P.M., Bondor,J.A., Swiderek,K.M. and dePaoli-Roach,A.A. (1991) Molecular cloning and expression of the regulatory (R_{GL}) subunit of glycogen-associated protein phosphatase. *J. Biol. Chem*., **266**, 15782–15789.

Tu,J. and Carlson,M. (1995) REG1 binds to protein phosphatase type 1 and regulates glucose repression in *Saccharoymes cerevisiae*. *EMBO J*., **14**, 5939–5946.

Tu,J. Song,W. and Carlson,M. (1996) Protein phosphatase type 1 interacts with proteins required for meiosis and other cellular processes in *Saccharomyces cerevisiae*. *Mol. Cell. Biol*., **16**, 4199–4206.

Van Eynde,A., Beullens,M., Stalmans,W. and Bollen,M. (1994) Full activation of a nuclear species of PP1 by phosphorylation with protein kinase A and casein kinase 2. *Biochem. J*., **297**, 447–449.

Van Eynde,A., Wera,S., Beullens,M., Torrekens,S., Van Leuven,F., Stalmans,W. and Bollen,M. (1995) Molecular cloning of NIPP-1, a nuclear inhibitor of protein phosphatase-1, reveals homology with polypeptides involved in RNA processing. *J. Biol. Chem*., **270**, 28068–28074.

Wera,S. and Hemmings,B.A. (1995) Serine/threonine protein phosphatases. *Biochem. J*., **311**, 17–29.

Williams,K.R., Hemmings,H.C., LoPresti,M.B., Konigsberg,W.H. and Greengard,P. (1986) DARPP-32: primary structure and homology with protein phosphatase inhibitor-1. *J. Biol. Chem.*, **261**, 1890–1903.

Zhou,M.M. *et al*. (1995) Structure and ligand recognition of the phosphotyrosine binding domain of SHC. *Nature*, **378**, 584–592.

Zhu,L., Harlow,E. and Dynlacht,B.D. (1995) p107 uses a p21CIP1-related domain to bind to cyclin/cdk2 and regulate interactions with E2F. *Genes Dev*., **9**, 1740–1752.

Received on October 17, 1996; revised on December 6, 1996